Scaling law for the transient behavior of type-II neuron models

M. A. D. Roa and M. Copelli*
Laboratório de Física Teórica e Computacional, Departamento de Física, Universidade Federal de Pernambuco, 50670-901 Recife, PE, Brazil

O. Kinouchi
Faculdade de Filosofia, Ciências e Letras de Ribeirão Preto, Universidade de São Paulo, Avenida dos Bandeirantes 3900, 14040-901, Ribeirão Preto, SP, Brazil

N. Caticha
Instituto de Física, Universidade de São Paulo 05508-090, São Paulo, SP, Brazil
(Received 19 June 2006; revised manuscript received 23 October 2006; published 20 February 2007)

We study the transient regime of type-II biophysical neuron models and determine the scaling behavior of relaxation times τ near but below the repetitive firing critical current, $\tau \simeq C(I_c - I)^{-\Delta}$. For both the Hodgkin-Huxley and Morris-Lecar models we find that the critical exponent is independent of the numerical integration time step and that both systems belong to the same universality class, with $\Delta = 1/2$. For appropriately chosen parameters, the FitzHugh-Nagumo model presents the same generic transient behavior, but the critical region is significantly smaller. We propose an experiment that may reveal nontrivial critical exponents in the squid axon.

DOI: 10.1103/PhysRevE.75.021911 PACS number(s): 87.19.La, 05.45.−a, 05.90.+m, 89.75.Da

I. INTRODUCTION

The search for biophysical models for information processing systems has led to a variety of model neurons which describe the dynamics of the membrane potential. Collective properties arise from their interaction through several possible architectures and types of couplings. These can be chemical, voltage-gated synapses, simpler proteic electrical connections, or even just electrical ephaptic interactions arising between neighboring nerve fibers. Maybe the most striking feature of a neuron is the threshold of the stimulus that separates spiking from nonspiking regimes. Spiking neurons generate telltale signatures which have served as the basis for frequency-dependent neural codes, an idea that can be traced back to the work of Adrian in the 1920s [1]. Although of paramount importance to neural dynamics, spike frequencies do not tell the complete story. Subtle computations may arise from subthreshold dynamics such as for examples in the early stages of the mammalian visual system, olfactory bulb, and cortex. In many cases the key to the information dynamics lies in the transients, either below the current threshold to generate action potentials or the threshold to generate infinite sequences of spikes. In this paper we investigate transient spike trains of single model neurons since this might have a bearing on the collective behavior, i.e., computational capabilities, of subthreshold assemblies of neurons.

A dynamical system approach reveals that universal bifurcation scenarios for the firing behavior appear irrespective of the specific membrane ion channels and microscopic details involved. Full characterization of these bifurcation routes is important for a deeper understanding of how they affect the firing behavior and possible implementation of neural codes. For example, it is now acknowledged that bistable behavior and the small range of firing frequencies in neurons that undergo subcritical Hopf bifurcations prevent a robust use of a pure frequency code.

The transient behavior of neuron models has not received much attention in either experimental or theoretical studies. In this paper we study the divergence of transient times in a class of conductance-based models and show that it follows a universal critical behavior. We propose an experiment that may test our theoretical predictions and discuss how neurons could employ transients for computational purposes.

II. TRANSIENTS IN TYPE-II MODELS

The Hodgkin-Huxley (HH) model is a biophysically motivated system of four coupled nonlinear differential equations that describe the dynamics of the membrane potential V of the squid giant axon (e.g., [2,3]):

$$C\frac{dV}{dt} = G_{\mathrm{Na}}m^3h(E_{\mathrm{Na}} - V) + G_{\mathrm{K}}n^4(E_{\mathrm{K}} - V) + G_L(E_L - V) + I(t),$$

$$\frac{dx_i}{dt} = \alpha_{x_i}(V)(1 - x_i) - \beta_{x_i}(V)x_i. \quad (1)$$

x_i stand for the three gate variables $x_i = m$, h, and n describing the activation of ionic channels and $\alpha_{x_i}, \beta_{x_i}$ are voltage-dependent transition rates [3]:

$$\alpha_m(V) = \frac{2.5 - 0.1V}{e^{(2.5-0.1V)} - 1},$$

$$\beta_m(V) = 4e^{-V/18},$$

$$\alpha_h(V) = 0.07e^{-V/20},$$

*Electronic address: mcopelli@df.ufpe.br

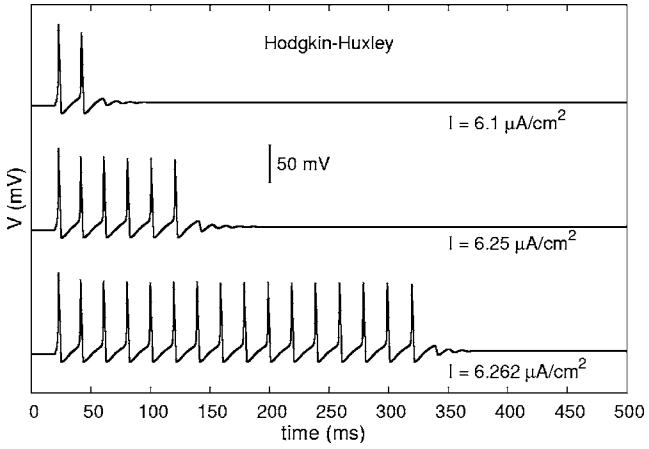

FIG. 1. Examples of transient behavior near I_c for the HH model. The constant step current is applied at $t=10$ ms. The estimated critical current is $I_c=6.264\,221\,256\,85\ \mu\mathrm{A/cm^2}$ for an integration time step $dt=0.01$ ms.

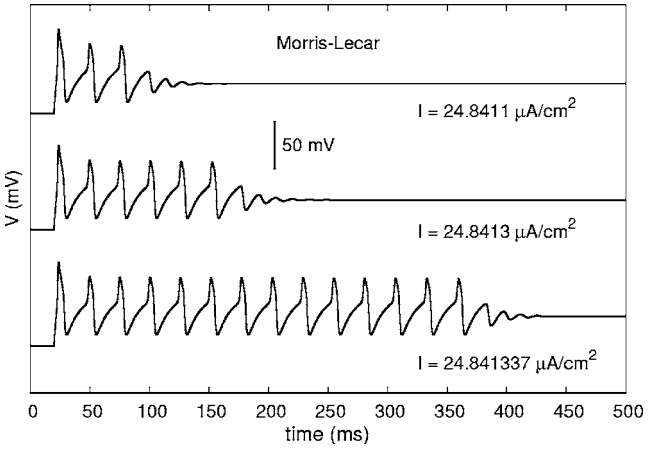

FIG. 2. Examples of transient behavior near I_c for the ML system. The constant step current is applied at $t=10$ ms. The estimated critical current is $I_c=24.841\,346\,762\,79\ \mu\mathrm{A/cm^2}$ for an integration time step $dt=0.01$ ms.

$$\beta_h(V)=\frac{1}{e^{(3-0.1V)}+1},$$

$$\alpha_n(V)=\frac{0.1-0.01V}{e^{(1-V)}-1},$$

$$\beta_n(V)=0.125e^{-V/20}, \tag{2}$$

where voltages are expressed in mV, rates in $\mathrm{ms^{-1}}$, $C=1\ \mu\mathrm{F/cm^2}$ is the specific membrane capacitance, $G_{\mathrm{Na}}=120\ \mathrm{mS/cm^2}$, $G_{\mathrm{K}}=36\ \mathrm{mS/cm^2}$, and $G_L=0.3\ \mathrm{mS/cm^2}$ are ionic conductances per unit area, and $E_{\mathrm{Na}}=115$ mV, $E_{\mathrm{K}}=-12$ mV, and $E_L=10.6$ mV are reversal potentials.

The HH system plays a fundamental role in the field of neurophysiology and computational neuroscience since it defines the class of conductance-based models. As a function of a constant applied current I, the HH model undergoes a subcritical Hopf bifurcation at $I=I_H$, above which the fixed point solution (membrane potential at rest) is no longer stable and trajectories are attracted to a stable limit cycle, leading to repetitive firing (infinite train of action potentials).

The sudden jump to a periodic behavior with nonzero frequency f is analogous to a first-order phase transition and is referred to as type-II behavior in the neuroscience literature [4]. As in first-order phase transitions, coexistence also appears in type-II behavior. Just below the Hopf bifurcation, the stable fixed point coexists with a stable limit cycle, their basins of attraction being separated by an unstable limit cycle [4]. Both limit cycles are created in a saddle-node (or "fold") bifurcation of cycles at $I=I_c<I_H$. In our analogy with equilibrium phase transitions, I_c would correspond to a spinodal point. If the fixed point at $I=0$ is perturbed by the application of a constant current near but below I_c, several spikes may appear before the system returns to the new resting state (Fig. 1).

In the original version of the Morris-Lecar (ML) model [5], a system with two coupled nonlinear ordinary differential equations (ODEs) used to describe action potentials in a barnacle motor fiber, the relevant bifurcation at the onset of repetitive firing is a saddle-node one. That means that the spiking frequency varies continuously from I_c as $f\propto(I-I_c)^{\beta}$, with $\beta=1/2$, which is similar to a mean field second-order phase transition behavior if we think of f as the order parameter. This transition is called type-I behavior in the neuroscience literature [4] and does not present a slow transient phenomenon similar to Fig. 1. However, the Morris-Lecar system has also been used to describe cells which present a type-II behavior [3,4], which occurs for the equations

$$C\frac{dV}{dt}=0.5G_{\mathrm{Ca}}\left[1+\tanh\left(\frac{V+1}{15}\right)\right](E_{\mathrm{Ca}}-V)+G_{\mathrm{K}}w(E_{\mathrm{K}}-V)+G_L(E_L-V)+I(t),$$

$$\frac{dw}{dt}=0.1\cosh(V/60)[1+\tanh(V/30)-2w], \tag{3}$$

when, for example, the values of the parameters are chosen as $G_{\mathrm{Ca}}=1.1\ \mathrm{mS/cm^2}$, $G_{\mathrm{K}}=2.0\ \mathrm{mS/cm^2}$, $G_L=0.5\ \mathrm{mS/cm^2}$, $E_{\mathrm{Ca}}=100$ mV, $E_{\mathrm{K}}=-70$ mV, and $E_L=-50$ mV. Then, large transient times are also observed (Fig. 2).

The FitzHugh-Nagumo (FHN) system

$$\frac{dV}{dt}=V(V-a)(1-V)-w+I,$$

$$\frac{dw}{dt}=\epsilon(V-\gamma w) \tag{4}$$

has been proposed as a low-dimensional toy model that represents the type-II behavior of the HH and other excitable systems. We verified that the transient behavior here reported is not seen with the usual parameters [6]. However, the FHN model can reproduce the HH transient behavior if one chooses parameters near $a=0.5$, $\gamma=4.2$, and $\epsilon=0.01$ (Fig. 3).

In this paper we show that the long relaxation times in type-II models are a consequence of the changes in phase space which occur near the creation of the limit cycles.

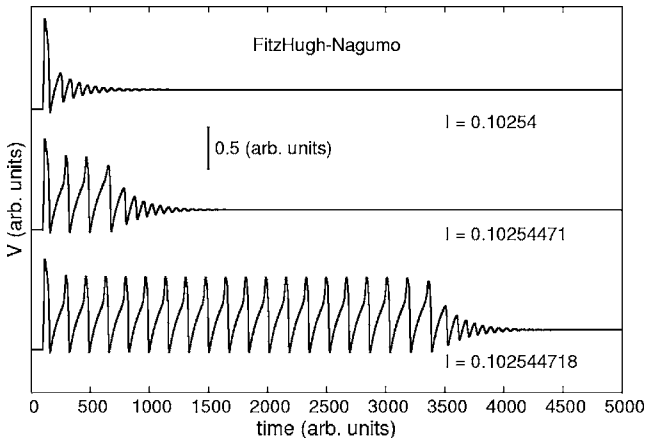

FIG. 3. Examples of transient behavior near I_c for the FHN system. The constant step current is applied at $t=10$. The estimated critical current is $I_c=0.102\,544\,718\,312\,7$ for an integration time step $dt=0.01$ (all quantities in arbitrary units).

Moreover, this leads to a scaling relation whose exponent can be predicted, in agreement with numerical simulations.

III. SCALING LAW

The relaxation time τ may be defined as the time until the last spike, or the time until the membrane voltage stays within a small distance from the resting potential (these two times are very similar near I_c). When we plot τ as a function of I_c-I we find a power law divergence of the relaxation time, $\tau \simeq C(I_c-I)^{-\Delta}$, where Δ is similar to a dynamic critical exponent. The Δ exponent characterizes the "critical slowing down" behavior near the bifurcation. We expect that Δ is a universal exponent but we are not aware that this exponent has been measured for neuron models. Here we report the measured exponents for these three type-II biophysical neuron models, finding very good agreement between them.

We integrated the equations using a standard fourth-order Runge-Kutta algorithm and determined τ by measuring the time interval from the onset of the current step to a near stop

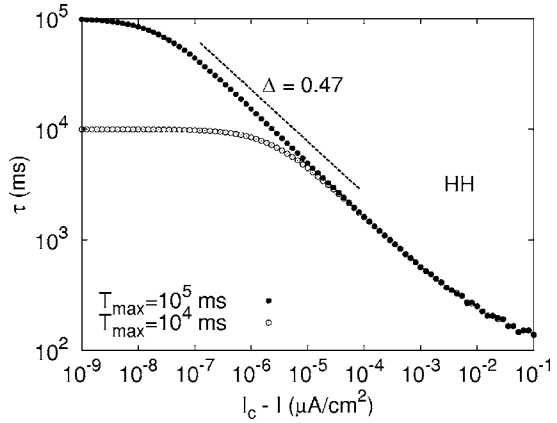

FIG. 4. Relaxation times for the HH model as a function of the distance to critical current for different integration times: $T_{max}=10^4$ (open circles) and 10^5 ms (filled circles).

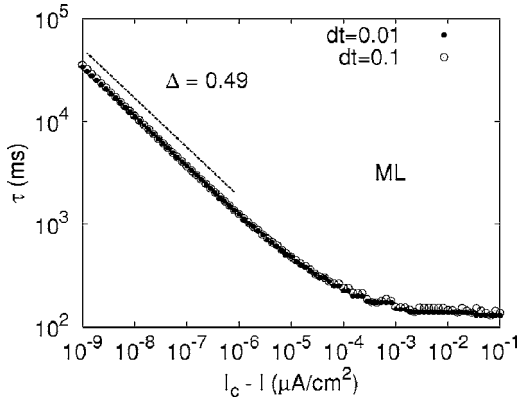

FIG. 5. Relaxation times for the Morris-Lecar model as a function of the distance to critical current for different integration times: $dt=0.01$ (filled circles) and 0.1 ms (open circles).

of the flow [$|\dot{\mathbf{x}}|<10^{-5}$, where $\dot{\mathbf{x}}$ is the velocity vector in phase space: $\dot{\mathbf{x}}=(\dot{w},\dot{v})$ for the ML and FHN systems, and $\dot{\mathbf{x}}=(\dot{w},\dot{m},\dot{h},\dot{n})$ for the HH model]. As opposed to the Hopf bifurcation, the fold bifurcation cannot be obtained analytically, so I_c was estimated numerically after integration of the ODEs up to a (long) maximum time T_{max}. The determination of the critical current is sensitive to T_{max}, but in practice this only limits the range of validity of the power law (see Fig. 4). We have employed $T_{max}=10^5$ ms and $dt=0.01$ ms, unless otherwise stated. The estimated critical currents $I_c(T_{max},dt)$ quoted in the figure captions are very precisely determined given T_{max} and the integration step size dt.

The critical exponent is determined from the plot τ vs I_c-I. We found $\Delta=0.47$ for the HH system (Fig. 4) and $\Delta=0.49$ for the ML model (Fig. 5), irrespective of the size of the integration step dt. This suggests a universal exponent $\Delta=1/2$. Obtaining long transients in the FHN model has proved numerically more difficult, since the phenomenon occurs only very close to I_c (Fig. 6). Nonetheless, we have obtained the exponent $\Delta=0.48$.

Figure 7(a) shows that for $I_c \lesssim I < I_H$ an unstable and a stable limit cycles coexist and surround a stable fixed point. The fixed point for $I=0$ lies outside both limit cycles [Fig.

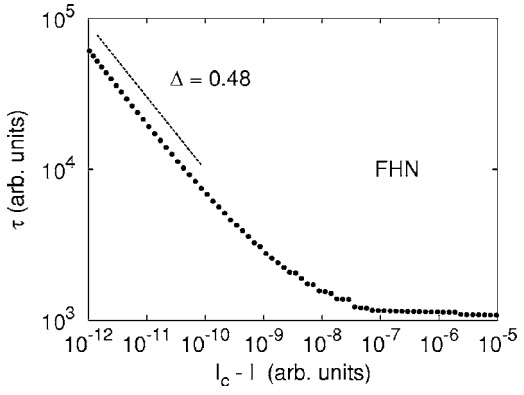

FIG. 6. Relaxation times for the FitzHugh-Nagumo model as a function of the distance to critical current. Note that the power law becomes visible only very close to the fold bifurcation ($I_c-I \sim 10^{-9}$).

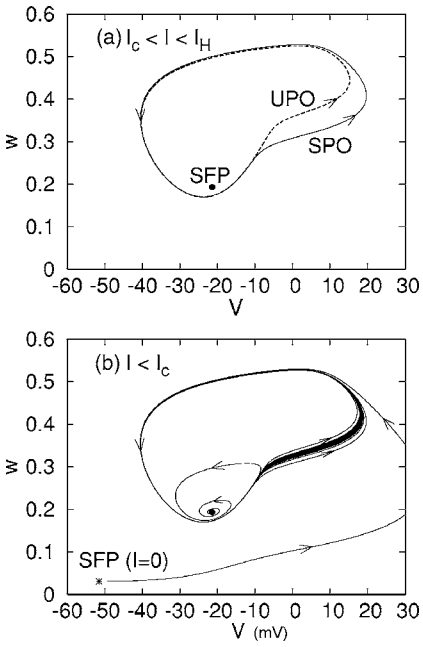

FIG. 7. Phase portraits of the ML model for I slightly above (a) and below (b) I_c. The long transient is dominated by the time it takes to pass through the region where the limit cycles are about to emerge. SPO (UPO)=stable (unstable) periodic orbit, SFP=stable fixed point.

7(b)]. Therefore, when the current is abruptly changed to $I \lesssim I_c$, the fixed point is displaced to a region within a "ghost limit cycle," and the transient is completely dominated by the time it takes for the system to overcome it. The ghost is a natural consequence of the system being immediately below a saddle-node bifurcation of cycles, and can be characterized by the vanishingly small flow component normal to the half-stable limit cycle that is created at $I=I_c$. It effectively works as a one-dimensional extended bottleneck through which the system must pass before reaching the fixed point (see Fig. 8 for a caricature). If one considers an analogous system in polar coordinates [7] $\dot{\theta}=f(r,\theta)$, $\dot{r}=\mu r$

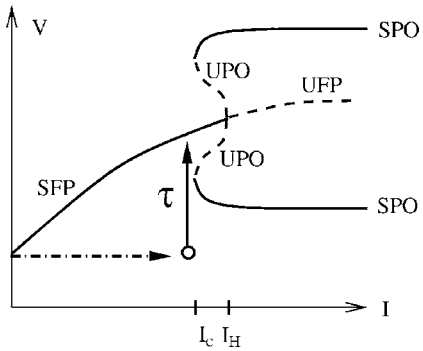

FIG. 8. Schematic bifurcation diagram for type-II neuron models. The fold bifurcation occurs at I_c, while the Hopf bifurcation occurs at I_H. Owing to the onset of the current step (dot-dashed arrow), the fixed point for $I=0$ becomes the initial condition in a new phase portrait. The transient τ (solid arrow) to reach the new fixed point is governed by the ghost limit cycle where the UPO and the SPO annihilate each other (see Fig. 7).

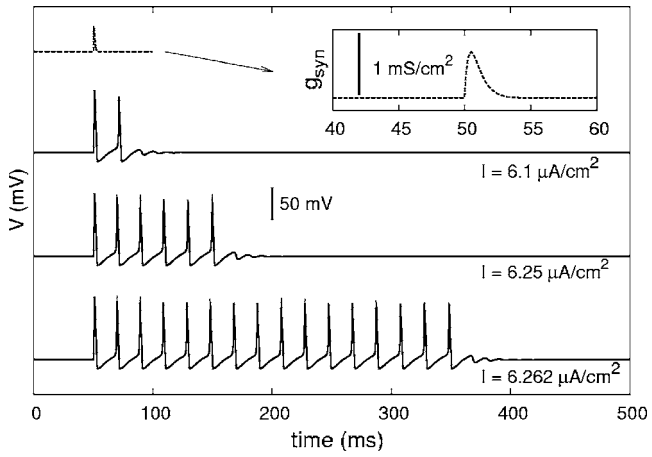

FIG. 9. Long transients appear if the system initially at rest with $I \lesssim I_c$ is perturbed by an additional EPSP (see text for details). Solid lines are membrane potentials, while the dashed line is the synaptic conductance.

$+r^3-r^5$, where $f(r,\theta)>0, \forall\ r>0$, it is clear that for $\mu \lesssim \mu_c=-1/4$ the time for the system to overcome the ghost at $r=1/2$ scales as $\tau \sim (\mu_c-\mu)^{-1/2}$ (the Hopf bifurcation occurring only at $\mu_H=0$). Solutions for the transient behavior have been obtained by Tonnelier [8] for McKean's piecewise linear version of the FHN model [9]. However, the scaling behavior has not been observed because the model has been studied in the absence of an external current.

It should be clear that the current step is just a simple way of putting the system outside the ghost limit cycle, but the scaling law for the transient is not restricted to this somewhat artificial protocol (even though it is very common in both theory and experiments). Close to the fold transition, any short-lived perturbation that is strong enough to make the system cross the ghost limit cycle will give rise to long transients back to the fixed point. We exemplify this with a biologically plausible example in the HH model. Suppose the system is somehow maintained close to criticality at $I \lesssim I_c$ (this could be achieved by several different possible mechanisms, so we just fix I). In addition, assume the neuron undergoes a fast excitatory postsynaptic potential (EPSP) simulated by an injected synaptic current $I_{syn}(t)=g_{syn}(t)(E_{\mathrm{Na}}-V)$:

$$C\frac{dV}{dt} = G_{\mathrm{Na}}m^3h(E_{\mathrm{Na}}-V) + G_{\mathrm{K}}n^4(E_{\mathrm{K}}-V) + G_L(E_L-V) + I + I_{syn}(t). \quad (5)$$

The fast change in the synaptic conductance is given by Rall's alpha function [10]: $g(t')=\theta(t')(g_m t'/\tau_s^2)\exp(-t'/\tau_s)$, where θ is the Heaviside function, $g_m=1$ mS/cm^2, $\tau_s=0.5$ ms, and $t'=t-t_{EPSP}$, where $t_{EPSP}=50$ ms is the time the EPSP is initiated. Results are shown in Fig. 9, whose similarity with Fig. 1 attests to the robustness of the effect (notice however that, differently from Fig. 1, in Fig. 9 the resting membrane potential is at the $I\neq 0$ fixed point *before* the perturbation). This opens interesting possibilities from the point of view of neuronal computation: the length of the transient response of a neuron "probed" by an EPSP could code for its

internal state of excitability, that is, for how close it is to I_c. Naturally, this transient coding would work only if the system is close to the fold bifurcation. We therefore could have another example in neuroscience of optimal information processing at criticality [11–17].

It is interesting to point out that this bottleneck effect is analogous to what occurs for type-I neurons above the saddle-node bifurcation that leads to repetitive firing. In that case, however, the ghost results from the annihilation of fixed points (not limit cycles) and the period T of the limit cycles diverges as $(I-I_c)^{-1/2}$. This provides a complementary scenario connecting both classes of neurons: the transient of type-II models below I_c diverges with the same exponent as the period of type-I models above I_c, that is, $\Delta=\beta$.

IV. CONCLUDING REMARKS

We were unable to find a description of this scaling law behavior for transients in neuron models or the associated dynamic critical exponent in the literature. Some kind of critical slowing down for subthreshold oscillations has been reported experimentally in the squid axon [18], but these authors examined the vicinity of a parametric subcritical Hopf bifurcation, not a saddle-node bifurcation of cycles induced by external currents. We propose that a similar experiment with high-precision injected currents near I_c could be used to check the power law found in the computational model. Since the area of the giant squid axon is of order ~ 1 cm^2, to examine the critical regime requires that current fluctuations should be less than $\sim 10^3$ pA (see Fig. 4). Even if the full critical regime seems to be hard to achieve, the initial divergence in the transient lifetime may provide an experimental check of our predictions.

We emphasize that both in standard experiments and in our single-compartment model space clamping is used. It might happen though, as in spin systems, that for the extended real system without voltage clamp, or for a compartmental model with a large number of compartments, the exponents may differ from the values here reported, changing the universality class to one not described by a "mean field" approach. Interestingly, this would mean that collective properties within a nontrivial universality class could be observed at the level of a single axon. So whether this result can be verified experimentally hinges on the effects that spatially extended neurons may have on the robustness of this picture.

Furthermore, noise could always play a role. In studies of type-I intermittency in simple maps, the length of the "laminar phase" $\langle l\rangle$ in a chaotic regime is analogous to the transient in this work and diverges as $\langle l\rangle \sim \epsilon^{-1/2}$ because of a zero-dimensional bottleneck as the distance ϵ to a tangent bifurcation tends to zero [19,20]. In the presence of additive noise with amplitude g [21], the scaling changes to $\sqrt{\epsilon}\langle l\rangle \sim f(g^2/\epsilon^{3/2})$, where f is a universal function (see also [22] for recent extensions). It is conceivable that similar scaling relations could be obtained for τ provided that the chaotic phase of intermittency theory could be replaced by some mechanism of "reinjection" in type-II neuron models. For instance, in the phenomenon of coherence resonance [23] noise itself plays this reinjecting role. However, the excitable systems employed are usually not close enough to the fold transition to exhibit long transients, so it would be interesting to investigate the effects of the scaling laws we report here in the resonance curves. These theoretical issues should be dealt with before engaging in an experimental search.

ACKNOWLEDGMENTS

The research was supported by FACEPE, CNPq, and the special program PRONEX. M.A.D.R. thanks the organizers of LASCON, the Latin American School on Computational Neuroscience, for financial support. M.C. thanks J. R. Rios Leite and J. R. L. de Almeida for inspiring discussions.

[1] E. D. Adrian, J. Physiol. (London) **61**, 49 (1926).
[2] D. Johnston and S. M.-S. Wu, *Foundations of Cellular Neurophysiology* (MIT Press, Cambridge, MA, 1995).
[3] C. Koch, *Biophysics of Computation* (Oxford University Press, New York, 1999).
[4] J. Rinzel and B. Ermentrout, in *Methods in Neuronal Modeling: From Ions to Networks*, 2nd ed. edited by C. Koch and I. Segev (MIT Press, Cambridge, MA, 1998), pp. 251–292.
[5] C. Morris and H. Lecar, Biophys. J. **35**, 193 (1981).
[6] J. Rinzel, in *Research Notes in Mathematics Nonlinear Diffusion*, edited by W. E. Fitzgibbon and H. R. Walker (Pittman Press, London, 1977), pp. 186–212.
[7] S. H. Strogatz, *Nonlinear Dynamics and Chaos: with Applications to Physics, Biology, Chemistry and Engineering* (Addison-Wesley, Reading, MA, 1997).
[8] A. Tonnelier, SIAM J. Appl. Math. **63**, 459 (2002).
[9] M. P. McKean, Adv. Math. **4**, 209 (1970).
[10] H. R. Wilson, *Spikes, Decisions and Actions: Dynamical Foundations of Neuroscience* (Oxford University Press, Oxford, 1999).
[11] S. Camalet, T. Duke, F. Jülicher, and J. Prost, Proc. Natl. Acad. Sci. U.S.A. **97**, 3183 (2000).
[12] J. M. Beggs and D. Plenz, J. Neurosci. **23**, 11167 (2003).
[13] D. R. Chialvo, Physica A **340**, 756 (2004).
[14] V. M. Eguíluz, D. R. Chialvo, G. A. Cecchi, M. Baliki, and A. V. Apkarian, Phys. Rev. Lett. **94**, 018102 (2005).
[15] L. S. Furtado and M. Copelli, Phys. Rev. E **73**, 011907 (2006).
[16] O. Kinouchi and M. Copelli, Nat. Phys. **2**, 348 (2006).
[17] D. R. Chialvo, Nat. Phys. **2**, 301 (2006).
[18] G. Matsumoto and T. Kunisawa, J. Phys. Soc. Jpn. **44**, 1047 (1978).
[19] P. Manneville and Y. Pomeau, Phys. Lett. **75A**, 1 (1979).
[20] Y. Pomeau and P. Manneville, Commun. Math. Phys. **74**, 189 (1980).
[21] J. E. Hirsch, B. A. Huberman, and D. J. Scalapino, Phys. Rev. A **25**, 519 (1982).
[22] H. L. D. de S. Cavalcante and J. R. Rios Leite, Phys. Rev. Lett. **92**, 254102 (2004).
[23] A. S. Pikovsky and J. Kurths, Phys. Rev. Lett. **78**, 775 (1997).